Journal of Photochemistry and Photobiology A: Chemistry 198 (2008) 18–25

Contents lists available at ScienceDirect

Journal of Photochemistry and Photobiology A: Chemistry

journal homepage: www.elsevier.com/locate/jphotochem

Porphyrin/calixarene self-assemblies in aqueous solution

Pavel Kubát[a,*], Kamil Lang[b,**], Pavel Lhoták[c], Pavel Janda[a], Jan Sýkora[a], Pavel Matějíček[d], Martin Hof[a], Karel Procházka[d], Zdeněk Zelinger[a]

[a] J. Heyrovský Institute of Physical Chemistry, v.v.i., Academy of Sciences of the Czech Republic, Dolejškova 3, 182 23 Praha 8, Czech Republic
[b] Institute of Inorganic Chemistry, v.v.i., Academy of Sciences of the Czech Republic, 250 68 Řež, Czech Republic
[c] Institute of Chemical Technology, Technická 5, 166 28 Praha 6, Czech Republic
[d] Department of Physical and Macromolecular Chemistry, Faculty of Science, Charles University, Hlavova 2030, 128 40 Praha 2, Czech Republic

ARTICLE INFO

Article history:
Received 21 December 2007
Accepted 10 February 2008
Available online 15 February 2008

Keywords:
Cationic porphyrin
Calix[4]arene
Thiacalix[4]arene
Sulfonylcalix[4]arene
Photophysics
Self-assemblies
Electron transfer

ABSTRACT

The variations of calix[4]arene linkages between phenolic units and of the cationic substituents on the porphyrin periphery affect modes of interaction and photophysical parameters of porphyrin/calixarene complexes. 5,10,15,20-Tetrakis(*N*-methylpyridinium-2-yl)porphyrin (TMPyP2) forms stable complexes with tetrasulfonated calix[4]arene, thiacalix[4]arene and sulfonylcalix[4]arene of the 1:1 stoichiometry with the binding constants above 10^6, $(9.3 \pm 0.9) \times 10^5$ and $(8.3 \pm 0.8) \times 10^4$ M^{-1}, respectively. We suggest that quenching of the singlet and triplet states of TMPyP2 involves fast electron transfer between excited singlet and triplet porphyrin states and phenolates. Surprisingly, both 5,10,15,20-tetrakis(*N*-methylpyridinium-4-yl)porphyrin (TMPyP4) and 5,10,15,20-tetrakis(4-trimethylammoniophenyl)porphyrin (TMAPP) behave differently. After binding of calixarenes nonspecific extended self-assemblies with a random arrangement of the porphyrin units are formed as confirmed by UV–vis, fluorescence spectroscopy, AFM, fluorescence microscopy and light scattering techniques. The TMPyP4/calix[4]arene system is the exception because both components form a molecular complex with the 1:1 stoichiometry. The complex is quickly transformed into extended self-assembly at higher TMPyP4 concentrations.

1. Introduction

Noncovalent intermolecular interactions play a dominant role in molecular recognition phenomena. In this respect, calixarenes have received considerable attention and have been applied in diverse areas such as catalysis, enzyme mimics, host–guest chemistry, selective ion transport, and sensors due to their complex abilities, conformational flexibility, and reactivity [1]. Calixarenes are used as potential building blocks for construction of supramolecular assemblies with suitable guest molecules like porphyrins. Depending on a guest molecule, different types of interactions are involved (ionic, cation–π, hydrogen bonding, hydrophobic, etc.). *para*-Sulfonato-calix[4]arene (CLX) (Fig. 1) has the advantage of being highly water-soluble while keeping the bowl-shaped conformation with hydrophilic upper and lower rims separated by a hydrophobic mid-region. This combination is suited for binding of various molecules like trimethylanilinium [2,3], tetramethylammonium [4], different macrocycles [5], amino acids, oligopeptides and acetylcholine with practical consequences for biological applications [6]. The binding process is mostly driven by enthalpy resulting mainly from the tight inclusion of the nonpolar part of a guest into the hydrophobic cavity of calixarene, and also by a favorable entropy gain due to desolvation of the charged groups upon ionic interaction. The sulfonate groups of calixarene can serve as anchoring points for positively charged guests and stabilize a complex.

Tetrasulfonated thiacalix[4]arenes (CLXS) and sulfonylcalix[4]arenes (CLXSO2) (Fig. 1) belong to a family of water-soluble calixarenes with a shape apparently homologous with that of calixarenes [7,8]. Sulfur-containing bridges impose changes in electronic and structural characteristics resulting in a wider cavity, lower electron density, and higher flexibility when compared with the methylene-linked cavity of calix[4]arene. The thia- and sulfonyl-analogues have higher complexation ability toward some organic molecules and metal ions in a solution owing to higher acidity of the phenolic OH groups and to the ligation of the bridging sulfur-containing groups.

Optical and photoactive properties predetermine porphyrins as efficient photosensitizers in many artificial light-harvesting systems [9]. Supramolecular architectures based on porphyrins, in

Abbreviations: TMPyP4, 5,10,15,20-tetrakis(*N*-methylpyridinium-4-yl)porphyrin; TMPyP2, 5,10,15,20-tetrakis(*N*-methylpyridinium-2-yl)porphyrin; TMAPP, 5,10,15,20-tetrakis(4-trimethylammoniophenyl)porphyrin; CLX, calix[4]arene; CLXS, thiacalix[4]arene; CLXSO2, sulfonylcalix[4]arene; AFM, atomic force microscopy; RLS, resonance light scattering; DLS, dynamic light scattering; SLS, static light scattering.

* Corresponding author. Tel.: +420 266 053 047; fax: +420 286 591 766.
** Corresponding author. Tel.: +420 266 172 193.
E-mail addresses: pavel.kubat@jh-inst.cas.cz (P. Kubát), lang@iic.cas.cz (K. Lang).

1010-6030/$ – see front matter © 2008 Elsevier B.V. All rights reserved.
doi:10.1016/j.jphotochem.2008.02.010

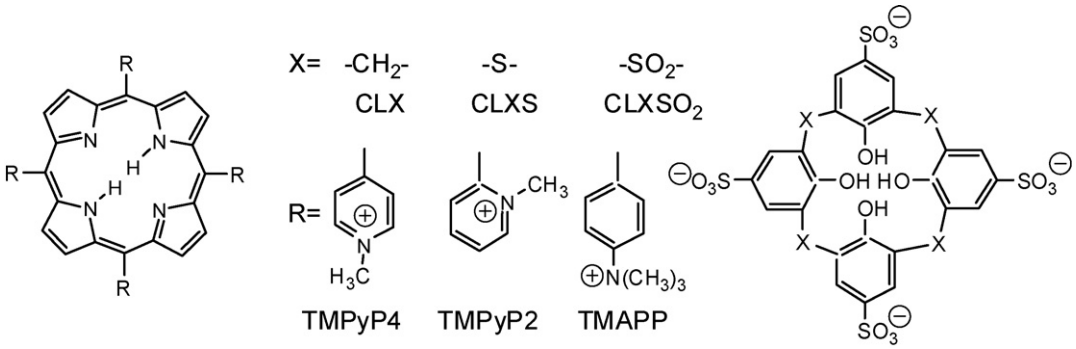

Fig. 1. Structure of porphyrins and calixarenes.

which interacting components are preorganized *via* non-covalent linkages, are particularly appealing since they open the way to a new rational synthesis of porphyrin arrays and functional systems with specific photophysical, optical, binding or magnetic properties. In this respect, calixarenes bearing negative charge (e.g., sulfonate groups) are potentially versatile synthons in aqueous solutions because they attract multicationic porphyrins primarily by ionic interactions. Such binding is usually accompanied by electronic interactions between the components leading to a change of overall photophysical properties [10]. Thus, the photoinduced electron transfer occurring between CLX and 5,10,15,20-tetrakis(*N*-methylpyridinium-4-yl)porphyrin (TMPyP4) was suggested [11]. Tetracationic Zn(II) porphyrins and tetraanionic sulfonated calix[4]arenes assemble into cage-like complexes and can serve as a model of the heme-protein active site [12,13]. The modulation of the structure and stoichiometry of multi-porphyrin species was achieved by a rational combination of sulfonated calix[4]arene with cationic TMPyP4 and its metallocomplexes [14–16]. This assembling leads to the formation of stable porphyrin self-aggregates in aqueous solution with a well-defined and tunable stoichiometry. The molecular organization of TMPyP4 in films is also characterized by the well-defined structure [17].

In this paper the structure and properties of porphyrin/calixarene complexes were modified by introducing different calixarene linkages between the phenolic units and/or porphyrin peripheral substituents. We show that the subtle frontier between a single complex and extended self-assemblies is controlled by the type of porphyrin and/or sulfonated calixarene.

2. Materials and methods

2.1. Chemicals

The tetratosylate salts of 5,10,15,20-tetrakis(*N*-methylpyridinium-4-yl) porphyrin (TMPyP4), 5,10,15,20-tetrakis(4-trimethylammoniophenyl)porphyrin (TMAPP, both Aldrich) and 5,10,15,20-tetrakis(*N*-methylpyridinium-2-yl)porphyrin (TMPyP2, Porphyrin Systems, Germany) were used as received. Calix[4]arene-*p*-tetrasulfonate (CLX) [18], thiacalix[4]arene-*p*-tetrasulfonate (CLXS) [19] and sulfonylcalix[4]arene-*p*-tetrasulfonate (CLXSO2) [20] were prepared according to the previously published procedures.

2.2. Absorption spectroscopy

The UV–vis absorption spectra were recorded using a PerkinElmer Lambda 19 and PerkinElmer Lambda 35 spectrometers. All experiments were conducted in 20 mM phosphate buffer (pH 7.0 ± 0.1) by adding aliquots of stock solutions at room temperature (25 °C). The affinity of porphyrins towards calixarenes was deduced mainly from the changes of the porphyrin Soret absorption bands. The shape and location of the Soret band are extremely sensitive to the changes in the microenvironment of the porphyrin moiety and enable better characterization of porphyrin structures than the Q-bands and/or fluorescence emission spectra. The titration data over the entire spectra were analyzed to obtain globally optimized parameters by singular value decomposition and nonlinear regression modeling using the Specfit program (Spectrum Software Associates, Inc.). The stoichiometry of TMPyP2 complexes was determined by the Job method of continuous variations.

2.3. Steady-state fluorescence and resonance light scattering (RLS)

The fluorescence and RLS spectra were measured on a PerkinElmer LS 50B luminescence spectrophotometer. All fluorescence emission spectra were corrected for the characteristics of the detection monochromator and photomultiplier using the fluorescence standards. The samples were excited at the $Q_y(1,0)$ absorption band (~520 nm) because it is less influenced by binding than the Soret band. The fluorescence quantum yields were estimated by the comparative method using solutions with matching absorbances at the excitation wavelength. The RLS experiments were conducted using simultaneous scans of the excitation and emission monochromators through the range of 300–600 nm.

2.4. Time-resolved fluorescence

The fluorescence decay curves were recorded on a 5000U Single Photon Counting setup (IBH, Glasgow, UK) using an IBH laser diode NanoLED-440L (440 nm peak wavelength, pulse width <200 ps, 1 MHz maximum repetition rate) and a cooled Hamamatsu R3809U-50 microchannel plate photomultiplier. The curves were recorded at a maximum of the steady-state emission spectrum of individual systems. Additionally, a 500 nm cutoff filter was used to eliminate scattered light. The data were collected in 2048 channels (0.052 ns per channel) till the peak value reached 10,000 counts. The decay curves were fitted to multiexponential functions (one, two or three exponential components were used) using the iterative reconvolution procedure of the IBH DAS6 software.

2.5. Laser flash photolysis

Laser flash photolysis experiments were performed using a Lambda Physik FL 3002 dye laser (412–440 nm, output 0.05–3 mJ/pulse, pulse width 28 ns). The transient spectra (300–800 nm) were recorded using a laser kinetic spectrometer LKS 20 (Applied Photophysics, UK). The time profiles of the triplet state decay were recorded at 460–480 nm using 250 W Xe lamp equipped

with a pulse unit, and a R928 photomultiplier (Hamamatsu). The lifetimes of the porphyrin triplet states (τ_T) were obtained by single exponential fitting to decay curves measured in argon-saturated solutions. The quantum yields of the triplet states (Φ_T) were estimated by the comparative method in air-saturated solutions that were adjusted to the same absorbance at the excitation wavelength.

2.6. Dynamic light scattering (DLS) and static light scattering (SLS)

The light scattering setup (ALV, Langen, Germany) consisted of a 633 nm He–Ne laser, an ALV CGS/8F goniometer, an ALV High QE APD detector and an ALV 5000/EPP multibit, multitau autocorrelator. Details on the SLS and DLS measurements of the aqueous solutions containing porphyrins are given elsewhere [21]. Solutions were prepared by adding of (i) 5 μL and (ii) 50 μL of 600 μM calixarene solutions into 1 mL of carefully filtered phosphate buffer (pH 7.1) in Eppendorf tubes. After it, 15 μL of 200 μM porphyrin solutions were added that corresponds to the porphyrin/calixarene molar ratios of 1:1 (3 μM each component) and 1:10. Finally, the prepared solutions were carefully poured immediately before the measurement into LS glass cells and were measured (i) 10 min and (ii) 24 h after mixing. The solutions of pure components and of higher concentrations of TMPyP4 and CLX (the molar ratio of 2:2, 6 μM each component) were also measured.

2.7. Microscopic techniques

Porphyrin/calixarene self-aggregates in the solid state were imaged by atomic force microscopy (Nanoscope IIIa, Veeco, USA) in a tapping mode. The samples were prepared by drop casting (20–50 μL) onto the basal plane of a mica substrate. The droplet was removed after 60 s and the substrate was dried in ambient air.

Fluorescence lifetime imaging (FLIM) measurements were carried out on an inverted epifluorescence confocal microscope MicroTime 200 (Picoquant, Germany). We used configuration containing a pulsed diode laser (LDH-P-C-405, 405 nm, Picoquant) providing 80 ps pulses at 40 MHz repetition rate, dichroic mirror 505DRLP, long-pass filter LP500 (Omega Optical), water immersion objective (1.2 NA, 60×) (Olympus), and detector PDM SPAD (MPD, USA). A module Picoharp 300 (Picoquant, Germany) recorded the photon events in a TTTR mode enabling the reconstruction of the lifetime histogram for each pixel [22]. In order to minimize the pile-up effects low power of 1.5 μW at the back aperture of the objective was chosen.

3. Results

Porphyrins TMPyP2, TMPyP4 and TMAPP (Fig. 1) stay monomeric in aqueous solutions as documented by literature data [11,23–26] and by respective absorption spectra with the narrow and intense Soret bands of the molar absorption coefficients above 2×10^5 M^{-1} cm^{-1} (Figs. 2–4).

3.1. Interaction of TMPyP2 with calixarenes

The addition of calixarenes to an aqueous solution of TMPyP2 results in a hypochromicity (6% for CLX, 20% for CLXS and CLXSO2)

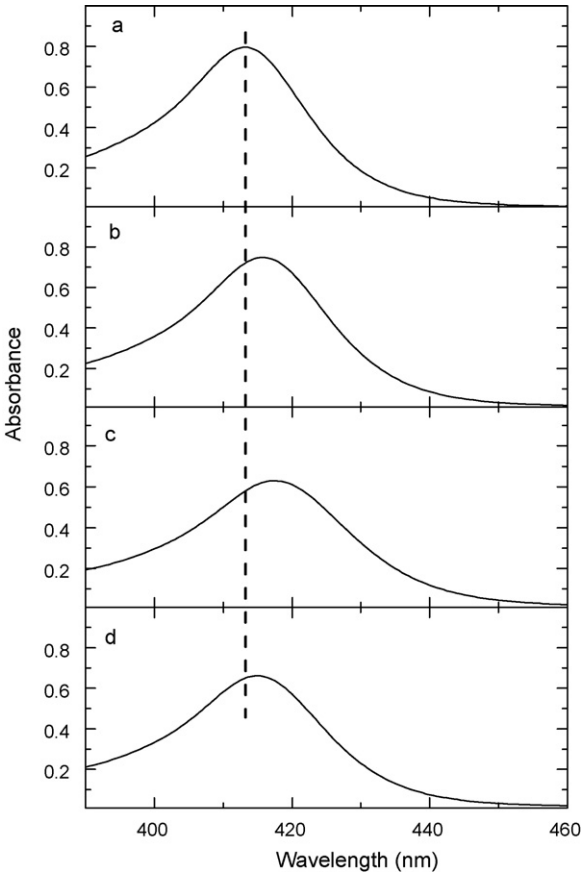

Fig. 2. The Soret band of 3.5 μM TMPyP2 (a) in the presence of 57 μM CLX (b), 46 μM CLXS (c) and 30 μM CLXSO2 (d). 20 mM phosphate buffer, pH 7.1.

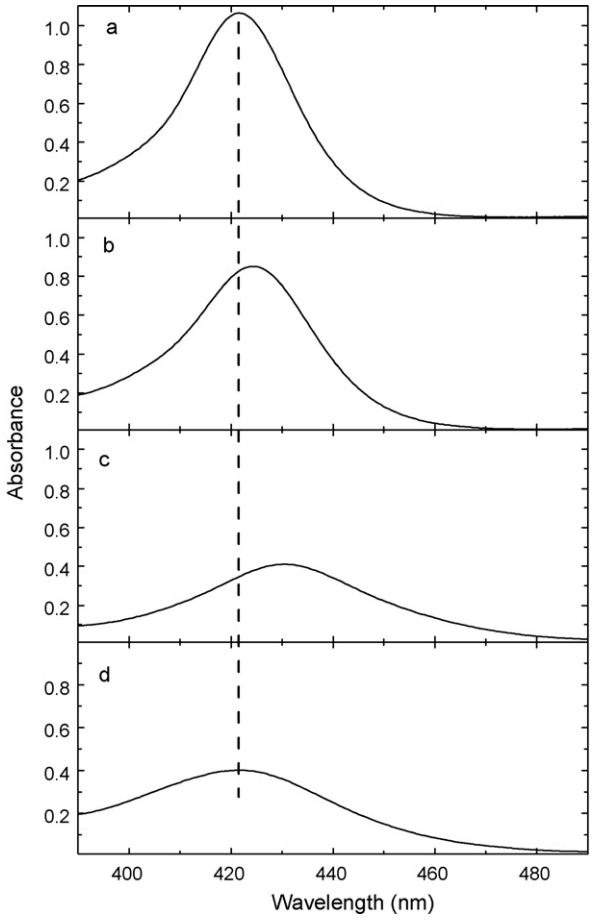

Fig. 3. The Soret band of 4.9 μM TMPyP4 (a) in the presence of 92 μM CLX (b), 69 μM CLXS (c) and 55 μM CLXSO2 (d). 20 mM phosphate buffer, pH 7.1.

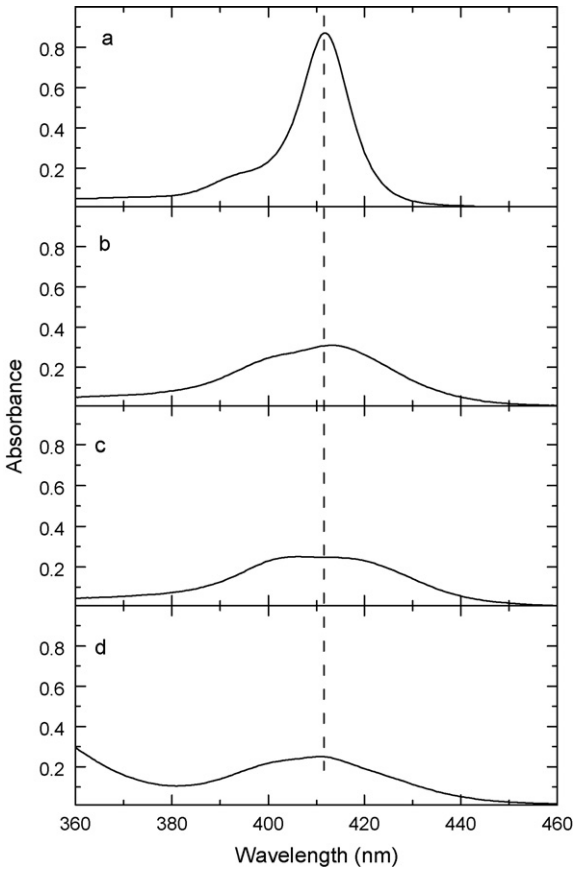

Fig. 4. The Soret band of 2.0 μM TMAPP (a) in the presence of 57 μM CLX (b), 46 μM CLXS (c) and 30 μM CLXSO2 (d). 20 mM phosphate buffer, pH 7.1.

and a small red shift (3 nm for CLX and CLXSO2, 5 nm for CLXS) of the original Soret band (Fig. 2) with the appearance of a well-defined isosbestic point in the Soret region. It indicates binding of TMPyP2 with studied calixarenes. The results of light scattering measurements (RLS, SLS and DLS) exclude self-aggregation of TMPyP2 and/or of TMPyP2/calixarene complexes. The binding constants extracted from the UV–vis titration experiments can provide further insight into the properties of formed complexes. The binding isotherms of TMPyP2/CLX exhibit a sharp saturation beyond the molar concentration ratio TMPyP2:CLX = 1:1 indicating high affinity of TMPyP2 towards CLX expressed by a binding constant above $10^6\ M^{-1}$. The titration data of the TMPyP2/CLXS and TMPyP2/CLXSO2 pairs were submitted to a singular value decomposition procedure using a global analysis routine. The results indicate the contribution of two spectral eigenvectors corresponding to unbound TMPyP2 and TMPyP2/calixarene complex. These results together with the maxima of the Job plots at the mole fraction of 0.5 confirm the 1:1 stoichiometry of the complexes. The least-squares fit of the data, assuming the 1:1 complexation model, gives the binding constants $K_b = (9.3 \pm 0.9) \times 10^5$ and $(8.3 \pm 0.8) \times 10^4\ M^{-1}$ for CLXS and CLXSO2, respectively.

Binding of calixarenes was also evidenced by fluorescence emission spectroscopy. The calixarene addition is accompanied by a reduction of the fluorescence quantum yields (Table 1) whereas the features of the fluorescence spectra are not changed. The fluorescence of TMPyP2 decays monoexponentially with a lifetime of 14.5 ns (Table 1). In the presence of equimolar CLX or CLXS the decay curves are best characterized by two lifetimes around 13 and 1 ns. The result reflects the equilibrium of two porphyrin species in the solution. The long-lived component belongs to unbound TMPyP2 while the 1 ns component can be assigned to TMPyP2/calixarene complexes. The short lifetime of the complex is in accordance with quenching of fluorescence emission upon binding of TMPyP2. Calixarene CLXSO2 has a minor effect on fluorescence decay kinetics that can be explained by a low contribution of the bound porphyrin (~17%).

Whereas the features of the triplet–triplet absorption spectra of TMPyP2 are not changed upon addition of CLX, CLXS and CLXSO2, the amplitudes of the triplet state signals decrease, i.e. the quantum yields of the triplet states (Φ_T) are reduced (Table 1). The Φ_T values related to TMPyP2 itself are equivalent to those of Φ_F and evidently reflect fast quenching of the excited singlet states as shown above.

Table 1
Photophysical properties of porphyrins (3 μM) in the absence and presence of calixarenes (3 μM) measured in 20 mM phosphate buffer, pH 7.1

System	Fluorescence			Triplet states	
	λ_{max} (nm)	τ_F (ns)	Φ_F	τ_T (μs)	Φ_T
TMPyP2/–	642, 708	14.5[a] (13.8[b])	(0.086[b])	610 (1160[b])	1.00[c]
TMPyP2/CLX	642, 708	12.0, 0.85[d]	0.021	37	0.29[c]
TMPyP2/CLXS	642, 708	14.0, 1.4[d]	0.038	30	0.45[c]
TMPyP2/CLXSO2	642, 708	13.9[a]	0.069	103	0.79[c]
TMPyP4/–	712[h]	5.1[a] (6.0[b], 4.9[e])	(0.047[b])	150 (170[b])	(0.89[e])
TMPyP4/CLX	712[h]	4.4, 1.7[d]	0.032	88	0.53 (0.57)[e]
TMPyP4/CLXS	712[h]	4.7, 0.83[d]	0.016	150	0.22
TMPyP4/CLXSO2	715[h]	5.0, 0.80[d]	0.016	120	0.50
TMAPP/–	647, 705	9.3[a] (9.3[f])	(0.070[f])	470 (540[f])	(0.80[f])
TMAPP/CLX	654, 709	8.3, 2.1, 0.63[g]	0.011	310	0.27
TMAPP/CLXS	655, 709	6.3, 2.1, 0.57[g]	0.015	370	0.22
TMAPP/CLXSO2	649, 705	9.3, 1,5, 0.54[g]	0.025	370	0.33

Maxima of fluorescence emission bands λ_{max}, fluorescence quantum yields Φ_F, fluorescence lifetimes τ_F, lifetimes of the triplet states τ_T in oxygen-free solution, and quantum yields of the triplet states Φ_T. Literature values are added in parentheses.

[a] Single exponential decay.
[b] Ref. [23].
[c] Relative values; Φ_T of TMPyP2 is taken to be 1.00.
[d] Best fitted by the two exponential function.
[e] Ref. [11].
[f] Ref. [24].
[g] Best fitted by the three exponential function.
[h] Broad band with a shoulder at about 670 nm.

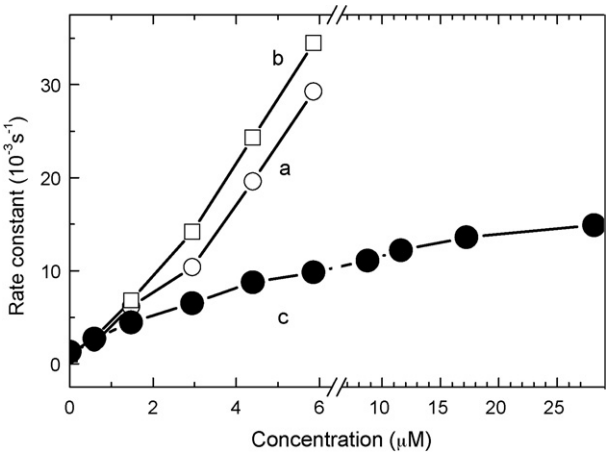

Fig. 5. Dependence of the rate constants of TMPyP2 triplet states deactivation on calixarene concentration of CLX (a), CLXS (b) and CLXSO2 (c). The traces were recorded at 460 nm in argon-saturated phosphate buffer, pH 7.0, excitation at 425 nm, fixed TMPyP2 concentration (6.0 μM), concentration of calixarenes varies from 0 to 30 μM.

In addition, an increasing concentration of calixarenes leads to a shortening of the triplet state lifetimes while the corresponding decay curves remain purely monoexponential (Fig. 5). This behavior points to an additional quenching process of the collisional origin that directly includes the porphyrin triplet states. A smaller quenching effect of CLXSO2 (Fig. 5c) is given by a low binding constant of TMPyP2/CLXSO2 complex (see above).

The extensive search for identification of a photoproduced transient turned to be unsuccessful in the presence of CLXS and CLXSO2. A possible explanation is that the transient lifetime is too short to be measured by our laser flash photolysis set-up and/or that its respective absorption band overlaps with the absorption band of the porphyrin triplet states. In contrast, we found small absorption signals that can be attributed to a new transient in the region 440–480 nm of the TMPyP2/CLX system (molar ratio 1:8 and more). Absorption of the transient recorded at 440 nm (Fig. 6b), where the contributions of triplet state absorption and ground state bleaching are cancelled off, rises with a comparable rate constant to that of the TMPyP2 triplet states decay (Fig. 6a). The transient decays monoexponentially and its lifetime is 1.8 ms regardless of CLX concentration (Fig. 6c). The transient is not observed after saturation a solution with oxygen.

3.2. Interaction of TMPyP4 with calixarenes

We have already shown that TMPyP4 forms the 1:1 complex with CLX characterized by the binding constant of $(6.4 \pm 0.9) \times 10^5$ M^{-1} [11]. Similarly to TMPyP2, binding is accompanied by a shift of the Soret band (Fig. 3b), and by quenching of both singlet and triplet states (Table 1). The dilute TMPyP4/CLX (1:1, 3 μM each component) solutions scatter light only weakly (Table 2) and the corresponding resonance light scattering (RLS) profiles are equivalent to those of the pure solvent (Fig. 7a) indicating that the particle fraction due to self-assembling of both components is very low if any. The scattering intensity increases about three times after 24 h standing in dark while the same system with 10-fold molar excess of CLX (1:10) behaves as a pure solvent. These results document a slow formation of TMPyP4/CLX self-assemblies under certain concentration conditions. To address this point we studied more concentrated solutions. Indeed, double concentrated solutions of TMPyP4/CLX (6 μM each component) exhibit a pronounced light scattering intensity due to extensive aggregation as

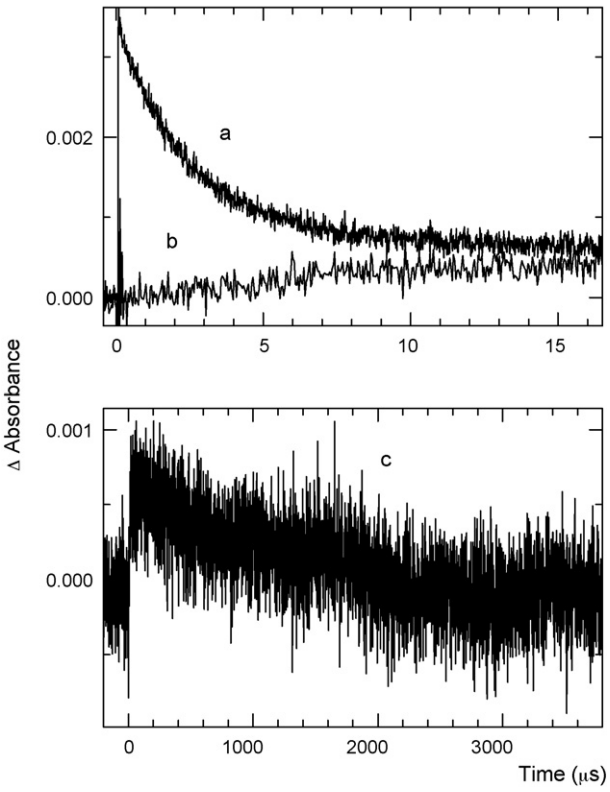

Fig. 6. Time-resolved absorbance changes at 460 nm (a) and 440 nm (b and c) after excitation by a 425 nm laser pulse in air-saturated 20 mM phosphate buffer, pH 7.1. 3 μM TMPyP2 and 300 μM CLX, average of 200 traces.

particles with R_H close to 300 nm are created immediately after component mixing.

Both CLXS and CLXSO2 cause large hypochromicity and broadening of the Soret band of TMPyP4 (Fig. 3c and d). The Soret band is red-shifted by 9 nm in the presence of CLXS while CLXSO2 practically does affect the band position. The spectral changes are accompanied by the decrease of the fluorescence emission intensity and can be explained by the formation of TMPyP4/CLXS or TMPyP4/CLXSO2 aggregates as it is further corroborated by light scattering measurements (see below). The fluorescence decay curves are characterized by two lifetimes; the component around 5 ns belongs to unbound TMPyP4 and the short-lived component is

Table 2
Light scattering characterization of porphyrin/calixarene assemblies in freshly prepared aqueous solutions (10 min after mixing)

System	R	R_H (nm)	I_{LS} (a.u.)[a]	R	R_H (nm)	I_{LS} (a.u.)[a]
TMPyP2/CLX	1:1	–	1	1:10	–	1
TMPyP2/CLXS	1:1	–	2	1:10	–	1
TMPyP2/CLXSO2	1:1	–	3	1:10	–	1
TMPyP4/CLX	1:1	127	6	1:10	–	1
TMPyP4/CLX	2:2	287	419	–	–	–
TMPyP4/CLXS	1:1	430	283	1:10	282	405
TMPyP4/CLXSO2	1:1	473	240	1:10	496	507
TMAPP/CLX	1:1	611	160	1:10	646	154
TMAPP/CLXS	1:1	596	525	1:10	591	260
TMAPP/CLXSO2	1:1	510	319	1:10	583	204

Porphyrin/calixarene molar ratio R, hydrodynamic radii R_H, and intensity of light-scattering I_{LS}. Measured in 20 mM phosphate buffer, pH 7.1.

[a] Extrapolated value to the zero scattering angle; the I_{LS} value for pure aqueous solutions is ca. 1 a.u.

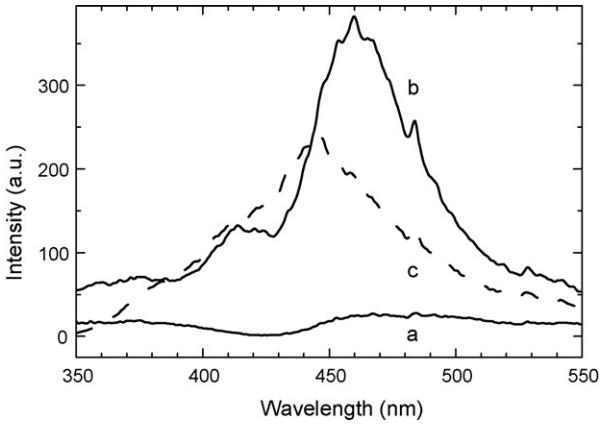

Fig. 7. RLS spectra of 3.0 μM TMPyP4 in the presence of 37 μM CLX (a), CLXS (b) and CLXSO2 (c, dashed line). 20 mM phosphate buffer.

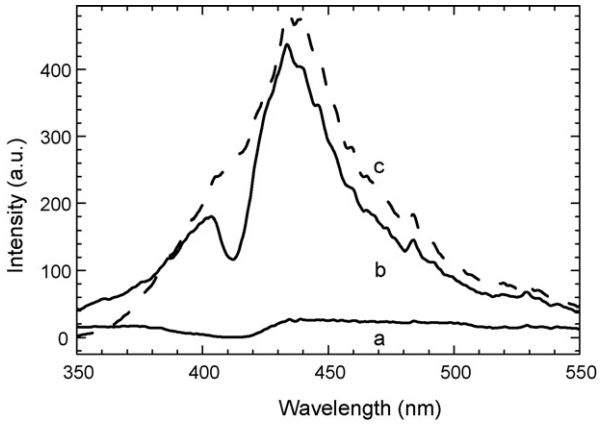

Fig. 8. RLS spectra of 2.4 μM TMAPP in the absence (a) and presence of 2.5 μM (b) and 37.5 μM CLXSO2 (c, dashed line). 20 mM phosphate buffer.

due to a combined effect of binding and calixarene-induced assembling. While the Φ_T values decrease, the lifetimes of the triplet states remain nearly unaffected.

The RLS technique allows for the identification of extended aggregated species even at low concentrations as aggregates with observable RLS contain a large number of electronically interacting monomer units [27]. The large RLS signals appear in the Soret region that is typical for the presence of large assemblies (Fig. 7b and c). Also light scattering measurements reveal a significant fraction of multimolecular assemblies. The hydrodynamic radii, R_H, and the intensities of light-scattering signals are listed in Table 2. The size of relatively large particles is practically unaffected by the ratio of the components and by the linkage of phenyls within calixarene molecules. The radii R_H increase several times after 24 h aging of the solutions. The importance of the component charges for the particle formation is evidenced by experiments at pH < 1 where no assembling occurs. Under these conditions porphyrin pyrrole nitrogens are protonated and repulsion between the porphyrin molecules overcomes attraction forces between porphyrin and calixarene. Evidently, different binding behavior of TMPyP2 and TMPyP4 towards calixarenes is affected by the location of methyl groups in the peripheral pyridinium substituents.

3.3. Interaction of TMAPP with calixarenes

The absorption spectra of TMAPP undergo marked changes in the presence of calixarenes. Strong hypochromicity and splitting of the Soret band to two peaks located around 403 and 420 nm and an increased absorption between 420 and 460 nm reveal extensive porphyrin assembling (Fig. 4). The similar absorption features were observed in aqueous solutions of TMAPP in the presence of inorganic salts [28,29]. These changes indicate self-stacking of TMAPP to higher aggregates. At molar ratios TMAPP/calixarene close to one, the presence of the TMAPP monomer can be still identified in the absorption spectra. Assembling is also documented by RLS and light scattering measurements. The RLS spectra, with a negative signal centered at 412 nm due to residual monomer self-absorption, are very intensive (Fig. 8). Light scattering experiments point to large particles with radii between 500 and 600 nm (Table 2). After 24 h the radii increase above 1000 nm. Because the radii of aggregates are fairly high, the Guinier condition ($R_g q \ll 1$, where R_g is the radius of gyration, and q is the magnitude of the scattering vector) is not probably fulfilled for all measured scattering angles. Assuming the validity of the Guinier rule, the obtained ratio R_g/R_H is in the range 0.8–1.0. For comparison, the monodisperse hard spheres have the R_g/R_H value of 0.778.

The concomitant effect of assembling is fluorescence quenching and the fact that fluorescence decay curves are best characterized by three components; one of them has lifetime below 1 ns (Table 1). In addition, the Φ_T values are significantly decreased (Table 1).

3.4. Characterization of self-assemblies by microscopic techniques

The particles were deposited on fresh mica surfaces and studied by AFM. In accordance with the above-described spectral and light scattering measurements, the solutions of TMPyP2 with CLX, CLXS or CLXSO2, and TMPyP4 with CLX did not contain any nanostructures. The AFM images show isolated spherical particles of TMPyP4 (Fig. 9a) and oval particles of extensively assembled TMAPP (Fig. 9b). The measurement is complicated by the fact that all particles are very soft. The TMPyP4/CLXSO2 system produces nanostructures with the diameters and heights ranging from 6 to 60 nm and 0.3 to 4.2 nm, respectively. The particles deposited from highly aggregated TMAPP/CLXS solutions are bigger having the diameter between 50 and 120 nm and the height about 1.5 nm. The measured sizes indicate that the particles flatten and collapse upon adsorption on the surface.

The spherical shape of porphyrin/calixarene assemblies is confirmed by the fluorescence imaging (Fig. 10a and b). The diameter of deposited particles is around 1 μm that is the size comparable with that obtained from light-scattering experiments. The fluorescence lifetimes of the porphyrin molecules embedded in assemblies are below 1 ns (Fig. 10c). Note, that the fluorescence lifetime of unbound TMPyP4 is 5.1 ns.

4. Discussion

The positive charges at the periphery of TMPyP4, TMPyP2 and TMAPP are responsible for electrostatic repulsive forces between porphyrin molecules preventing porphyrin aggregation in aqueous solutions [11,23–26]. However, it has been shown that the porphyrins self-aggregate strongly, provided that electrostatic repulsion of their peripheral groups is cancelled by complexation with hydrophobic or large counteranions [30,31] including sulfonated calixarenes [11,17].

The differences in interactions of the TMPyP2 and TMPyP4 positional isomers with calixarenes could be explained by steric effects and electron-accepting effects of pyridinium substituents including both inductive and mesomeric contributions [32]. From the structural point of view, the pyridinium substituents in TMPyP2 are sterically hindered by the porphyrin pyrrole rings whereas in TMPyP4 a lower degree of steric hindrance causes that the

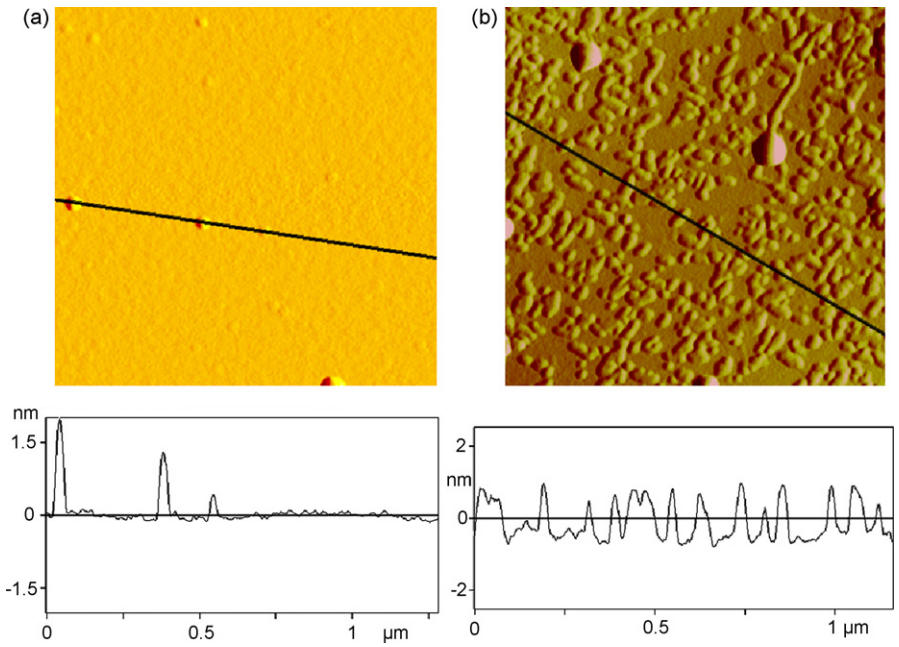

Fig. 9. Tapping mode AFM image (upper part) and line analysis (lower part) of nanostructures formed by drop casting of 4.0 μM TMPyP4 and 40 μM CLXSO2 (a) and 3.7 μM TMAPP and 29 μM CLXS (b) on mica substrate. Incubation time 1 h, area 1 μm × 1 μm.

substituents rotate relatively freely. All these factors contribute to differences between TMPyP2 that forms 1:1 complexes, and TMPyP4 that self-aggregate after binding with calixarenes. Reinhoudt and co-workers [12] described the formation of a cage-like complex between zinc(II) 5,10,15,20-tetrakis(*N*-methylpyridinium-3-yl)porphyrin and tetrasulfonated calix[4]arenes. The porphyrin moiety sits atop the calixarene upper rim due to a complementary charge distribution of both interacting components as the positive charges fit the size of the sulfonated calix[4]arene rim. The studied TMPyP2 complexes can be of a similar cage-like structure. It is possible that the extent of size matching of opposite charges affects the binding affinity of TMPyP2 towards CLX, CLXS and CLXSO2. In this respect, the binding constants decreasing in the order CLX > CLXS > CLXSO2 indicate that TMPyP2 fits the sulfonated rim of CLX considerably better than that of CLXSO2. A wider and more flexible cavity of CLXS and CLXSO2 results probably in worse matching of TMPyP2 and the calixarene sulfonated rim. We cannot preclude a contribution of a binding mode where TMPyP2 is attracted to the phenolate lower rim and other stoichiometries especially at molar excess of one of the component. However, we have no spectral indications of the stoichiometries different from 1:1. Similar arguments can explain lower affinity of TMPyP4 towards CLX when compared with TMPyP2. The positive charges TMPyP4 are more distant from each other than those of TMPyP2 and probably do not fit the negative charges on the upper calixarene rim so well.

The featureless Soret bands (Fig. 3c and d) and large RLS intensities (Fig. 7) of TMPyP4 solutions together with the particle formation show extensive self-assemblies in the presence of CLXS and CLXSO2. The ability to form self-assemblies increases in the order CLX < CLXS < CLXSO2 (Table 2). The acidity of phenolic OH groups increases in the same order [33]. Hence, both CLX and CLXS are pentaanions at pH 7.0 because the sulfonic groups attached to the upper rim and one phenolic group dissociate, and more acidic CLXSO2 is mainly octaanion. The increasing charge of the calix[4]arene unit is not fully compensated by one

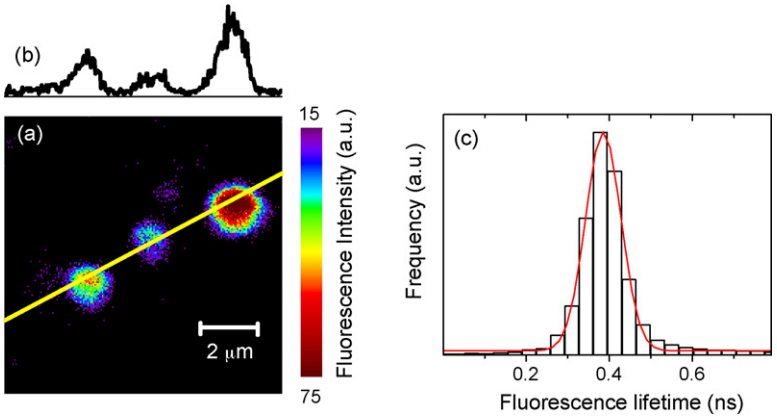

Fig. 10. Fluorescence intensity image of self-assemblies of TMPyP4 and CLXSO2 on a quartz substrate (a), fluorescence intensity along the marked line (b) and the histogram of determined fluorescence lifetimes (c). The corresponding Gaussian distribution fit yields the average lifetime of 0.39 ± 0.08 ns.

TMPyP4 molecule and this fact in conjunction with the effects of the pyridinium substituents causes the attachment of additional porphyrin and calix[4]arene molecules to form relatively large self-assemblies.

The tendency to form self-assemblies differs from that of TMPyP4/tetrasulfonated calix[4]arene system bearing carboxylic functions instead of the phenolate groups at the lower rim [14–16]. The originally formed supramolecular complex 1:4 with each of the methylpyridinium substituents oriented into the sulfonated upper rim undergoes further self-assembling depending on solution parameters. It leads to the formation of a series of discrete complexes having well-defined and tunable stoichiometries derived from the piling the porphyrin units above and below the plane of the central 1:4 porphyrin/calixarene complex to ultimately give a 7:4 TMPyP4/calix[4]arene complex. Evidently, the different binding modes are affected by the calix[4]arene structure.

The Soret bands of TMPyP4 and TMAPP assemblies do not exhibit distinct absorption features typical for organized structures such as are H- and J-aggregates [34]. Evidently, binding of the relatively large calixarene molecules prevents the organization of the monomer units into a closely interacting arrangement. Increased hydrophobicity along with more distant positive charges on the peripheral substituents of TMAPP can be responsible for a low tendency of TMAPP to form a discrete complex with calixarenes.

The formation of extended aggregates and/or binding of various molecules or structures have an enormous impact on photophysical properties and on the photosensitizing ability of porphyrins [10]. The fluorescence and triplet states quantum yields of aggregates are more than one order of magnitude lower than those of the corresponding monomeric porphyrins due to competitive relaxation processes [35]. In accordance with it, the formation of TMPyP4 and TMAPP assemblies is accompanied by strong decrease of fluorescence and triplet states amplitudes.

The fluorescence quantum yields and lifetimes of TMPyP2 in the calix[4]arene complex are effectively quenched indicating a competitive non-radiative process occurring within the complex. In addition, a shortening of the triplet state lifetimes points to a collisional quenching process that directly includes the porphyrin triplet states. In search for a possible quenching mechanism we exclude the energy transfer from excited singlet porphyrin to calixarenes. It would by a highly energetically unfavorable process because the calixarene excited singlet states are above the porphyrin S_2 states. On the other hand, electron transfer from the excited singlet states and triplet states of isomeric TMPyP4 to phenolates of CLX is an exothermic process and it is thermodynamically feasible [11]. To our best knowledge no data on redox couples of TMPyP2 are available, so we cannot estimate the thermodynamics of the electron transfer pathway in this case. We suggest that quenching of TMPyP2 involves fast electron transfer between excited singlet and triplet porphyrin states and phenolates. Our effort to detect a conceivable electron transfer product, i.e. ion pair $TMPyP2^{-\cdot}/PhO\cdot$, was successful in the TMPyP2/CLX system. The relatively long-lived transient is observed within 440–500 nm i.e., in the spectral region typical for phenoxyl radicals [36] and anion-radicals of porphyrins [37].

In summary, we have designed nine porphyrin/calixarene systems with different porphyrin substituents and/or calix[4]arene linkages to extend the possibilities of noncovalent syntheses of multi-porphyrin assemblies. These variations lead to different behavior strongly depending on the type of porphyrin substituents. The steady-state and time-resolved study of TMPyP4 and TMAPP after binding to calixarenes in solution reveals the formation of extended assemblies, in which nonradiative decay channels effectively quench the excited singlet and triplet states. Porphyrin TMPyP2 forms the stoichiometrically well-defined complexes with all calixarenes. The binding constants decrease in the series CLX > CLXS > CLXSO2 and we have suggested that it reflects the extent of size matching of opposite charge densities on the interacting pairs.

Acknowledgments

This research was supported by the Czech Science Foundation (Nos. 203/07/1424 and 203/06/1244) and by the Academy of Sciences of the Czech Republic (grant no. KAN100500652). JS and MH thank the Ministry of Education, Youth and Sports of the Czech Republic (LC06063). KP and PM thank the Marie Curie Research and Training Network (grant no. 505 027, POLYAMPHI) and long-term research plan of the Ministry of Education, Youth and Sports of the Czech Republic No. MSM 0021620857.

References

[1] C.D. Gutsche, in: J.F. Stoddart (Ed.), Calixarene Revisited: Monographs in Supramolecular Chemistry, The Royal Society of Chemistry, Cambridge, 1998.
[2] S. Shinkai, K. Araki, T. Matsuda, N. Nishiyama, H. Ikeda, I. Takasu, M. Iwamoto, J. Am. Chem. Soc. 112 (1990) 9053–9058.
[3] G. Arena, A. Casnati, A. Contino, G.G. Lombardo, D. Sciotto, R. Ungaro, Chem. Eur. J. 5 (1999) 738–744.
[4] J.L. Atwood, L.J. Barbour, P.C. Junk, G.W. Orr, Supramol. Chem. 5 (1995) 105–108.
[5] J.L. Atwood, L.J. Barbour, M.J. Hardie, C.L. Raston, Coord. Chem. Rev. 222 (2001) 3–32.
[6] F. Perret, A.N. Lazar, A.W. Coleman, Chem. Commun. (2006) 2425–2438.
[7] P. Lhoták, Eur. J. Org. Chem. (2004) 1675–1692.
[8] N. Morohashi, F. Narumi, N. Iki, T. Hattori, S. Miyano, Chem. Rev. 106 (2006) 5291–5316.
[9] P.D.W. Boyd, C.A. Reed, Acc. Chem. Res. 38 (2005) 235–242.
[10] K. Lang, J. Mosinger, D.M. Wagnerová, Coord. Chem. Rev. 248 (2004) 321–350.
[11] K. Lang, P. Kubát, P. Lhoták, J. Mosinger, D.M. Wagnerová, Photochem. Photobiol. 74 (2001) 558–565.
[12] R. Fiammengo, P. Timmerman, F. de Jong, D.N. Reinhoudt, Chem. Commun. (2000) 2313–2314.
[13] R. Fiammengo, K. Wojciechowski, M. Crego-Calama, P. Timmerman, A. Figoli, M. Wessling, D.N. Reinhoudt, Org. Lett. 5 (2003) 3367–3370.
[14] L. Di Costanzo, S. Geremia, L. Randaccio, R. Purrello, R. Lauceri, D. Sciotto, F.G. Gulino, V. Pavone, Angew. Chem. Int. Ed. 40 (2001) 4245–4247.
[15] G. Moschetto, R. Lauceri, F.G. Gulino, D. Sciotto, R. Purrello, J. Am. Chem. Soc. 124 (2002) 14536–14537.
[16] F.G. Gulino, R. Lauceri, L. Frish, T. Evan-Salem, Y. Cohen, R. De Zorzi, S. Geremia, L. Di Costanzo, L. Randaccio, D. Sciotto, R. Purrello, Chem. Eur. J. 12 (2006) 2722–2729.
[17] G. de Miguel, M. Pérez-Morales, M.T. Martín-Romero, E. Muñoz, T.H. Richardson, L. Camacho, Langmuir 23 (2007) 3794–3801.
[18] S. Shinkai, K. Araki, T. Tsubaki, T. Arimura, O. Manabe, J. Chem. Soc., Perkin Trans 1 (1987) 2297–2299.
[19] N. Iki, T. Fujimoto, S. Miyano, Chem. Lett. (1998) 625–626.
[20] N. Iki, T. Horiuchi, H. Oka, K. Koyama, N. Morohashi, C. Kabuto, S. Miyano, J. Chem. Soc., Perkin Trans. 2 (2001) 2219–2225.
[21] P. Kubát, K. Lang, P. Cígler, M. Kožíšek, P. Matějíček, P. Janda, Z. Zelinger, K. Procházka, V. Král, J. Phys. Chem. B 111 (2007) 4539–4546.
[22] P. Kapusta, M. Wahl, A. Benda, M. Hof, J. Enderlein, J. Fluoresc. 17 (2007) 43–48.
[23] K. Kalyanasundaram, Inorg. Chem. 23 (1984) 2453–2459.
[24] K. Kalyanasundaram, J. Chem. Soc., Faraday Trans. 2 (79) (1983) 1365–1374.
[25] K. Kano, H. Minamizono, T. Kitae, S. Negi, J. Phys. Chem. A. 101 (1997) 6118–6124.
[26] R.F. Pasternack, P.R. Huber, P. Boyd, G. Engasser, L. Francesconi, E. Gibbs, P. Fasella, G.C. Venturo, L. de C. Hinds, J. Am. Chem. Soc. 94 (1972) 4511–4517.
[27] P.J. Collings, E.J. Gibbs, T.E. Starr, O. Vafek, C. Yee, L.A. Pomerance, R.F. Pasternack, J. Phys. Chem. B 103 (1999) 8474–8481.
[28] K. Kano, M. Takei, S. Hashimoto, J. Phys. Chem. 94 (1990) 2181–2187.
[29] D.W. Dixon, V. Steullet, J. Inorg. Biochem. 69 (1998) 25–32.
[30] J. Mosinger, M. Janošková, K. Lang, P. Kubát, J. Photochem. Photobiol. A 181 (2006) 283–289.
[31] Z. Ou, H. Yao, K. Kimura, J. Photochem. Photobiol. A 189 (2007) 7–14.
[32] F.J. Vergeldt, R.B.M. Koehorst, A. van Hoek, T.J. Schaafsma, J. Phys. Chem. 99 (1995) 4397–4405.
[33] H. Matsumiya, Y. Terazono, N. Iki, S. Miyano, J. Chem. Soc., Perkin Trans. 2 (2002) 1166–1172.
[34] P. Kubát, K. Lang, K. Procházková, P. Anzenbacher Jr., Langmuir 19 (2003) 422–428.
[35] R.F. Khairutdinov, N. Serpone, J. Phys. Chem. B 103 (1999) 761–769.
[36] S. Steenken, P. Neta, J. Phys. Chem. 86 (1982) 3661–3667.
[37] P. Neta, J. Phys. Chem. 85 (1981) 3678–3684.